



RESEARCH MEMORANDUM

EFFECT OF DIAMETER OF CLOSED-END COOLANT PASSAGES
ON NATURAL-CONVECTION WATER COOLING
OF GAS-TURBINE BLADES

By Arthur N. Curren and Charles F. Zalabak

Lewis Flight Propulsion Laboratory
Cleveland, Ohio

NATIONAL ADVISORY COMMITTEE
FOR AERONAUTICS
WASHINGTON

January 24, 1956
Declassified October 31, 1958

NATIONAL ADVISORY COMMITTEE FOR AERONAUTICS

RESEARCH MEMORANDUM

EFFECT OF DIAMETER OF CLOSED-END COOLANT PASSAGES ON NATURAL-
CONVECTION WATER COOLING OF GAS-TURBINE BLADES

By Arthur N. Curren and Charles F. Zalabak

SUMMARY

An experimental investigation was conducted on a water-cooled gas turbine with blade coolant-passage diameters ranging from 0.100 to 0.500 inch, corresponding to length-to-diameter ratios from 25.5 to 5.1, in various quadrants of the turbine. The investigation was conducted to determine (1) whether coolant-passage length-to-diameter ratio has a significant effect on natural-convection heat-transfer correlation, and (2) whether turbine blade temperatures could be calculated with reasonable accuracy from a theoretical natural-convection heat-transfer correlation.

Because of large temperature gradients within liquid-cooled turbine blades, it was found necessary to account for the conduction process in order to determine the temperature difference between the coolant passage surface and the place of blade temperature measurement. By use of an electrical analog to make the conduction correction, it was found possible to calculate turbine blade leading-edge temperatures within about 15° F of the measured temperatures for a water-cooled blade operating at a temperature of approximately 300° F with coolant passages from 0.125 to 0.500 inch in diameter. A larger scatter in calculated temperatures resulted for the blade trailing edge with a passage diameter of 0.100 inch.

No significant differences in the heat-transfer results could be shown for the various length-to-diameter ratios investigated. For coolants that have very high heat-transfer coefficients, such as water, the blade temperatures can be calculated from the heat-transfer coefficients obtained from a theoretical natural-convection heat-transfer correlation without considering length-to-diameter ratio for values of this ratio from 25.5 to 5.1.

INTRODUCTION

The experimental investigation reported herein was made to determine the effect of closed-end coolant-passage length-to-diameter ratio

on the natural-convection heat-transfer characteristics of liquid-cooled turbines, and to determine whether blade temperature could be calculated with reasonable accuracy. A correlation of experimental natural-convection heat-transfer data with air as the coolant is reported in reference 1 for flat plates and large-diameter tubes with length-to-diameter ratios up to 5.0. In reference 2, this correlation satisfactorily describes the heat-transfer data for upward water flow in vertical tubes of length-to-diameter ratio as high as 40 when the water through-flow rate is sufficiently small. In references 3 and 4, heat-transfer investigations of a turbine with natural-convection water-cooled blades having closed-end coolant passages covered a range of coolant-passage diameters from 0.060 to 0.125 inch (corresponding to a length-to-diameter ratio range of 43.5 to 20.9). The coolant-passage heat-transfer coefficients calculated from the turbine data were much smaller than those indicated from the results of reference 1. Better agreement could be obtained if coolant-passage surface temperatures were used rather than the temperatures measured near the outer blade surface, as reported.

In a natural-convection liquid-cooled rotating turbine blade with closed-end coolant passages, the heated boundary layer adjacent to the coolant-passage wall flows radially inward, being replaced by cooler fluid flowing radially outward as a central core. Where the passages are small (large length-to-diameter ratio), the heated boundary layer could easily take up so much of the passage cross-sectional area that the circulation of coolant outward in the central core of fluid would be restricted. Where the flow is through tubes with large diameter with respect to length, no blockage due to boundary-layer thickness is expected. An analytical investigation reported in reference 5 shows that, for the conditions of the tests of references 3 and 4, the natural-convection cooling effects would be considerably decreased for coolant-passage diameters less than 0.146 inch. However, this conclusion is based on calculations using the previously mentioned outer surface temperatures. Use of coolant-passage surface temperatures in the calculation of the degree of blockage would result in the same conclusion but for a passage of smaller diameter.

In order to obtain additional information on the effects of coolant-passage length-to-diameter ratio on heat transfer and blade temperature for turbine blades cooled by natural-convection circulation of the coolant, an experimental liquid-cooled turbine was built. The coolant-passage diameters ranged from 0.100 to 0.500 inch, which corresponded to length-to-diameter ratios from 25.5 to 5.1. Since no suitable method of measuring blade coolant-passage surface temperatures was known at the time of fabrication, thermocouples were located near the coolant passages and an electrical analog was used to obtain empirical constants for correcting temperatures.

The turbine was operated with water as coolant over the following range of conditions:

Coolant-passage diameters: 0.100, 0.125, 0.250, 0.375, and 0.500 inch, corresponding to length-to-diameter ratios of 25.5, 20.4, 10.2, 6.8, and 5.1, respectively
Turbine inlet temperature: 600° to 1200° F
Coolant inlet temperature: 68° to 87° F
Turbine speed: 4000 to 10,000 rpm, corresponding to blade tip speeds of 245 to 611 feet per second and Grashof-Prandtl number products of the order of 10^{12}

The corrected temperature data were used to obtain heat-transfer correlations and were compared with analytically predicted blade metal temperatures. Calculated boundary-layer thicknesses together with the comparisons of calculated and measured blade temperatures were used to determine the extent of passage choking.

APPARATUS

The test setup of references 3 and 4 was retained for this investigation. The turbine is coupled to a dynamometer through a gearbox and combustion gas is supplied. The installation is shown in figure 1, and is described in detail in reference 3.

Turbine. - The present turbine (fig. 2) was designed with a thick blade cross section to permit coolant-passage diameters up to 0.500 inch. An airfoil shape was approximated by circular arcs in a manner that would permit ease in machining the blades on a single ring. As a result, the profile of these blades is not considered a good aerodynamic design. Blade chord and span were of the order of 2 and $2\frac{1}{2}$ inches, respectively. The turbine material was AISI-403 stainless steel.

As shown in figure 3, the turbine rotor was divided into quadrants of five blades each. All the blades had trailing-edge coolant passages of 0.100-inch diameter but the leading-edge coolant passages differed in each quadrant, having diameters of 0.125, 0.250, 0.375, or 0.500 inch. Hereinafter, the quadrants will be referred to as the 0.125-inch quadrant, 0.250-inch quadrant, and so forth. The quadrants were separated by dams in order that the heat rejected to the coolant from each quadrant could be separately measured.

Instrumentation. - Inlet-gas temperatures were measured by chromel-alumel thermocouples spaced in four equal radial increments along the blade span at circumferential positions 90° apart. The measurements were

made in a plane $1/4$ inch upstream of the nozzle blades (fig. 1). The coolant inlet temperature was measured by iron-constantan thermocouples where the coolant entered the turbine wheel (fig. 2).

Rotating chromel-alumel thermocouples measured all blade metal temperatures shown schematically in figure 4, and coolant temperatures at the tip of the leading-edge coolant passage (thermocouple 5) and at the coolant discharge (thermocouple 6). A rotating thermocouple pickup consisting of a slip-ring and brush system was utilized for transferring the electromotive force generated by the thermocouples to temperature-measuring equipment. The instrumentation indicated in figure 4 was duplicated in each of the quadrants, with the exception of thermocouple 4, which was located only in the 0.125- and 0.500-inch quadrants. Data are presented for thermocouples 2 and 4 only as indications of turbine blade body and extremity temperatures.

Thermocouples in the center of the leading-edge coolant passage at the blade tip were installed in the following manner. The 0.060-inch-diameter thermocouple tube, which enclosed the ceramic-insulated thermocouple at the tip of the tube, was held in position by means of a slot which extended along the surface of the coolant passage. This slot was formed by drilling a 0.062-inch-diameter hole parallel to the center line of the coolant passage and spaced so that the center line of the drilled hole was 0.025 inch from the coolant-passage wall. This spacing resulted in a "breakthrough" into the coolant passage, the width of the breakthrough being less than the 0.060-inch-diameter thermocouple tube. One-half inch of the sealed, temperature sensing end of the thermocouple tube was formed so that it was parallel to, but offset from, the remainder of the tubing by the distance between the center lines of the coolant passage and the drilled hole. The short transition section of the tube between the two parallel parts was then flattened to allow the sensing end of the tube to project from the slot into the coolant passage as the tube was slid along the installation slot to the desired radial position as determined by the radial length of the slot. To keep the sensing end of the tube centered in the coolant passage and provide minimum flow restriction, three wires of about 0.030-inch diameter were silver-soldered normal to the tube about $1/4$ inch from the end and extending to the coolant-passage wall in a manner to serve as spacing struts when the installation was complete.

Other rotating thermocouples were installed near the outer and inner rotor rim surfaces, as shown in figure 2. The angular position was midway between two adjacent blades in the 0.250-inch quadrant. The difference in temperature Φ between these two locations is an indication of the heat flow through the rotor rim.

EXPERIMENTAL PROCEDURE

Rig operation. - Turbine rotor speed was controlled by means of an electric dynamometer to which the rotor was connected through a gearbox. Power was either supplied or absorbed, as necessary, by the dynamometer to maintain a constant turbine speed during a particular run. The inlet temperature was controlled by varying the amount of fuel to the two direct-flow burners, while the air flow was maintained practically constant. A range of coolant flows was supplied to the turbine for each operating condition, and pertinent data were recorded at each weight flow.

Coolant temperature control. - The coolant temperature was controlled by regulating the coolant flow to the blades. The coolant flow supplied to the blades is not necessarily a measure of coolant circulation in the coolant passages, since the coolant is supplied to a reservoir in the blade base (figs. 1 and 2) and circulation occurs as a result of natural-convection forces. The primary effect of varying the coolant flow was to influence the temperature of the coolant entering the blade coolant passages by changing the mixture temperature in the reservoir.

Experimental range. - Table I summarizes the range of turbine operating conditions. The minimum coolant-flow requirement was established as just enough flow to prevent vaporization of coolant in the coolant passages. Since the turbine, owing to its unsymmetrical internal configuration, was dynamically balanced with all the coolant passages filled, vaporization of the coolant in the passages during operation would seriously affect this balance.

CALCULATION PROCEDURE

Heat flow. - The coolant temperature at the entrance to the rotor and the temperatures of the coolant in the discharge passages from each of the quadrants were measured. The heat-flow rate from each of the quadrants was calculated by the relation

$$Q_T = w_c c_p (T_6 - T_{c,in})$$

The symbols are defined in appendix A. It was assumed that the total measured coolant flow was divided equally among the quadrants. In the range of temperatures investigated, c_p for water was assumed to be 1.0. No corrections were made to account for the temperature rise of the coolant in bringing it to the rotational speed of the coolant outlet. For this reason the calculated heat flows are about 3 percent or less too high.

Since the calculated heat-flow rate Q_T represents the heat flow from the blade and from the rotor rim, a calculation of the heat flow from the rotor rim $Q_R = k_m A_R \Delta T / \tau_R$ was made. The average peripheral area was obtained in the following way: The area abcde bounded by the dashed lines in figure 2 was reduced in order to simulate the rotor rim by a parallel-walled plate. On a layout of this section, a line was faired through midpoints of the radial distances between the rotor rim ae and the surface in contact with the coolant bcd. The cross-sectional area between the rotor rim and this faired line was determined, then divided by the width of the rim. By subtracting the resulting dimension from the outer radius of the rim, an average radius for the faired line was obtained. The area A_R was then calculated as the surface area of a cylinder of length equal to the length of the faired line and of radius equal to the average radius of the faired line. The thickness τ_R for this equation was obtained by dividing the area abcde by the width of the outer rim of the rotor. In addition, the following assumptions were made: (1) temperatures are a distance τ_R apart; (2) temperatures from the thermocouples located in the 0.250-inch quadrant apply all around the rim; and (3) the cross-sectional area of the coolant passages can be neglected.

The heat flow through the rim Q_R was subtracted from the total heat flow Q_T in order to obtain the heat flow to the coolant from the blade only $Q_{B,T}$. For the conditions investigated, the heat flow through the rim was of the order of 10 percent of the total heat flow.

As a check of the heat-flow correction for conduction from the blade to the rim, a spanwise temperature distribution for the blade and rim section was determined by the analytical method of reference 6 in which temperature variations normal to the span were neglected. It was assumed that the temperature of the inner rim surface (bcd, fig. 2) was the same as the temperature of the coolant within the blade passage. The conduction heat flow was then calculated with the aid of the calculated temperature gradient at the blade base. For the point checked, the heat flow determined by the measured temperature gradient in the rim agreed within 30 percent of that calculated with the temperature gradient at the blade base. In addition, the heat transfer from the blade by conduction was found to be about 4 percent of that transferred to the coolant by convection. For this reason, the heat flow calculated from the rim temperature gradient was considered to be sufficiently accurate.

Blade-metal temperature for heat-transfer correlation. - Preliminary results indicated the necessity of using a coolant-passage surface temperature for heat-transfer correlations. A means was devised to determine surface temperatures from blade-body temperature measurements by using results from an electrical analog to describe the conduction

process. The construction and operation of the analog are described in appendix B. The surface temperature is implied by the equations for the temperature difference

$$T_1 - T_{i,le} = \frac{\psi_{le} Q_{B,le}}{2\pi k_m b} \ln \left(\frac{r_1}{r_{i,le}} \right)$$

and

$$T_3 - T_{i,te} = \frac{\psi_{te} Q_{B,te}}{2\pi k_m b} \ln \left(\frac{r_3}{r_{i,te}} \right)$$

which are the same as equation (2) in appendix B. The radii for these equations are now the radius of the coolant-passage surface and the radius of the thermocouple location in the actual blade. On X-ray photographs the distances were measured from the thermocouple bead to the coolant-passage surface. For both the leading and the trailing edge, this distance was 0.067 inch for all the quadrants. The temperatures T_1 and T_3 measured at the blade midspan were used because the spanwise temperature profile determined in the previous section was found to be essentially constant throughout the midspan region. Table II lists the correction factors ψ , which are defined in appendix B and were determined from the electrical analogs. No analog was constructed for the 0.375-inch quadrant. The heat flows $Q_{B,le}$ and $Q_{B,te}$ are the heat flows into the fluid in the coolant passages at the leading and trailing edges, respectively, and the sum is equal to the total heat flow $Q_{B,T}$. These heat flows were determined by the fractional division of the current flow through the leading- and trailing-edge sections of the analog (table II).

These electrical analogs were constructed with a resistance to simulate a constant outside heat-transfer coefficient. The effect of a variable heat-transfer coefficient is illustrated in reference 6. Temperature profiles were computed by relaxation methods for a cross section of a liquid-cooled turbine rotor blade. For the present report, the effect of the coefficient on the variation of the division of heat flow to the two coolant passages of reference 6 was determined. Where the coefficient was constant, 48 percent of the total heat flow to the blade was transferred to the coolant in the passage nearest the leading edge. With a peripheral variation of the coefficient, 50 percent of the total heat flow was transferred to the coolant in the leading-edge passage. Because the difference in division of heat flow was so small, the peripheral variation of outside heat-transfer coefficient was neglected for the purposes of this report.

Data correlation. - The blade-to-coolant heat-transfer coefficient was calculated as

$$h_i = \frac{Q_B}{A_i(T_i - T_5)}$$

where Q_B represents the heat flow to the coolant within the leading- or trailing-edge passage, as determined in the previous paragraph. The temperature of the coolant in the tip of the blade passage T_5 was used to represent a core temperature in the calculation of heat transfer for the following reasons. The geometry of the turbine is such that the water entering the reservoir has an angular velocity less than that of the water in the reservoir owing to the difference in radii between the coolant entry to the rotor cavity and to the reservoir. The dams dividing the various quadrants serve to bring the water to the rotor speed, and, in doing so, considerable mixing must take place. In addition, local turbulence due to heated water flowing radially inward from the blade passages promotes mixing in the reservoir. These conditions coupled with the observation that the temperatures T_5 and T_6 are not greatly different (see table I) justify the use of T_5 as the temperature of the water flowing radially outward in the blade passages. In any given blade, the coolant temperature at the tip of the trailing-edge passage was assumed to be the same as that in the leading-edge passage. The accuracy of this assumption will be discussed later.

While T_5 represents the best available value for the temperature of the fluid to which the heat is transferred, the outlet temperature T_6 is more often known in a design problem. If T_6 were used in the computation of heat-transfer coefficients, lower values of the coefficient would be calculated when T_5 becomes greater than T_6 . This condition might arise when the coolant passage is so small that the coolant flow rate in the passage is lessened by interference between the radially outward and inward flows.

Natural-convection heat-transfer data can be correlated on the basis of the relation (ref. 5)

$$Nu = f(GrPr)$$

The property values (refs. 7 and 8) of the coolant were evaluated at the film temperature $(T_i + T_5)/2$ (ref. 4). In the calculation of the Grashof number the gravity term was replaced by the acceleration term $\omega^2 r$. The radius r was taken as the radius to the midpoint of the coolant passage within the blade. The characteristic dimension l in the Nusselt and Grashof numbers was taken as the average length of the coolant passage, including the part in the rim. The temperature difference θ was that used for the heat transfer $T_i - T_5$.

Calculated blade temperatures. - Because of the high heat-transfer coefficients and heat-flow rates encountered in this investigation, the temperature difference between the wall surface and the coolant was small. If random errors occur in the temperature data, correlations involving small temperature differences are subject to scatter that is not representative of the actual temperature of the body under consideration. For this reason it was decided to calculate blade temperatures and compare them with the measured blade temperatures. It was assumed that the heat transfer in both coolant passages of all quadrants can be described by

$$Nu = 0.0210(GrPr)^{2/5}$$

which was developed in reference 5. The exponent of the Grashof-Prandtl numbers product involves the assumption that the passages are large enough that the heated boundary layer does not interfere with the flow into the passage. The numerical coefficient is the one resulting in the best fit of the equation with data obtained on vertical plates and cylinders in the range $10^{10} < GrPr < 10^{12}$. It is also shown in reference 1 that points determined from the form of this equation that describes the local coefficient agree quite well with data from experiments with turbulent free convection of air in a tube of $l/D = 5.0$ over a range $10^9 < GrPr < 3 \times 10^{12}$. In order to calculate the blade temperature, it is first necessary to evaluate the coolant-passage surface-to-coolant temperature difference θ from this equation, using the experimentally measured values of rotor speed, coolant temperature T_5 and heat flow rate Q_B , and fluid properties based on an assumed average of coolant and wall temperature. When a first approximation of θ has been determined for a given set of turbine data, a new approximation of the average of the coolant and wall temperature can be made. This is usually accurate enough to proceed with the calculation of θ . The temperature difference $T_1 - T_{i,le}$ or $T_3 - T_{i,te}$, which is necessary to the conduction of the measured heat flows, is then calculated with the analog corrections already described.

RESULTS AND DISCUSSION

Measured Temperature Data

In figure 5, the blade temperatures and the heat flow to the coolant for the 0.125- and the 0.500-inch quadrants are plotted against the flow rate of coolant supplied to the turbine for what is considered representative data. The calculated heat flow to the coolant on a per blade basis is included. The coolant flow rate is not necessarily the quantity of coolant that was circulated through the coolant passages. No large change

in the heat flow from the blade to the coolant occurred, although the coolant flow varied by a factor of 4. Neither the temperature level of the blade nor the coolant varied greatly with the range of coolant flows used. As mentioned previously, the primary effect of varying the quantity of coolant supplied to the turbine was to vary the coolant temperature in the reservoir in the rotor rim by mixing with the coolant that had circulated through the passages and removed heat from the blades. Figure 5 illustrates the degree of mixing of the coolant in the reservoir and the temperature rise within the passages by the agreement of the two coolant temperatures. The temperature of the coolant at the blade tip T_5 is 50° F higher than the outlet temperature T_6 in the 0.125-inch quadrant and only 10° F higher in the 0.500-inch quadrant. It can be seen in table I that, for the 0.375- and 0.250-inch quadrants, T_5 is not more than 20° F higher than T_6 . For even the 0.125-inch quadrant, the coolant temperature T_5 should therefore be adequate for heat-transfer correlations, in view of the heated entrance length and the rapid rise of the coolant temperature to a uniform value.

As shown in figure 5, the difference in temperature between the coolant and the lowest recorded blade temperature is on the order of 30° to 90° F. Because the coolant-passage surface temperature is certainly lower than any of the measured blade temperatures and the measured temperature differences between the coolant and the blade are so small, small changes in the metal temperature used would result in large changes in the temperature difference and, hence, equally large percentage changes in the heat-transfer coefficients. It is therefore necessary that the passage surface temperature be determined as accurately as possible for heat-transfer correlations. An electrical analog was constructed to determine the coolant-passage surface temperature by establishing the temperature drop between the thermocouple location and the coolant-passage surface due to the blade metal conduction process.

Corrected Temperature Data

Analog corrections. - Figure 6 is a plot of temperature differences between the blade metal and the coolant for the data of figure 5(a). The dip in the curves in the coolant flow range of 0.012 is probably the result of the particular variation of the coolant inlet temperature and the effective gas temperature, which can be noted in table I. In terms of heat-transfer correlations, it can be seen that the temperature difference obtained by analog corrections will result in Grashof numbers 60 to 40 percent of those calculated from the measured temperature difference. Correspondingly, the Nusselt number will be 1.7 to 2.5 times greater than obtained with the measured temperature difference.

Heat-transfer correlation. - A typical heat-transfer correlation obtained with corrected temperatures is shown in figure 7. For simplicity, the calculations for this figure were based upon relatively few data points believed to be representative of the entire data schedule. The data chosen were for the blade quadrants having the minimum and maximum leading-edge coolant-passage diameters, the 0.125- and 0.500-inch quadrants, respectively, a nominal effective gas temperature of 800° F, intermediate coolant flows from 0.0082 to 0.0126 pound per second per blade, and minimum and maximum turbine speeds of 4000 and 10,000 rpm, respectively, as shown in table I. The blade temperatures measured by thermocouples 0.067 inch from the coolant passage (thermocouples 1 and 3 in fig. 4) were corrected by the electrical-analog factor to obtain the coolant-passage surface temperature. Data corrected in this manner are shown to scatter about the correlation line theoretically predicted from reference 5 for natural convection. It is obvious that the percentage scatter is much greater than for any one blade-metal temperature in figure 5. It appears possible, however, that the theoretical correlation line from figure 7 can be used for predicting natural-convection heat transfer. Because the experimental temperature differences are small (fig. 6), any calculated heat-transfer coefficient equal to or larger than the experimental coefficient would be expected to result in calculated coolant-passage surface temperatures not much different from the coolant temperature. Inasmuch as the temperature difference between the coolant-passage surface and the coolant resulting from the analog corrections is so small that small errors in temperature measurements result in disproportionately large errors in the temperature difference, it is impossible to determine an exact heat-transfer correlation for the installation used in this investigation.

Blade Temperature Comparisons

Thus far, it has been shown that small errors in metal temperature can result in very large errors in calculated heat-transfer coefficients for liquid-cooled blades. It follows that, because of the small temperature differences between coolant and coolant-passage surface in liquid-cooled blades, large errors in an assumed value of heat-transfer coefficient should result in only a small error in a calculated blade temperature based on this heat-transfer coefficient. It was therefore assumed that blade-to-coolant heat-transfer coefficients could be represented by the theoretical correlation line of figure 7 for all coolant-passage diameters investigated herein. With the use of these blade-to-coolant heat-transfer coefficients, the measured coolant temperature T_5 , the measured heat flows apportioned by the fraction shown in table II, and the electrical-analog corrections from the coolant-passage surface temperature to the blade metal temperature at the thermocouple location, turbine blade temperatures were calculated and compared with experimentally measured temperatures. The complete data range for the 0.250-inch quadrant

was considered as typical for this comparison. Arbitrarily selected data were used for the comparisons in the 0.125- and 0.500-inch quadrants. The results are shown in figures 8 and 9.

Calculated turbine-blade leading-edge temperatures. - Figure 8(a) shows the calculated blade temperatures in the vicinity of the leading-edge coolant passage (thermocouple 1 in fig. 4) for a passage diameter of 0.125 inch. The calculated blade temperatures average about 15° F lower than the measured temperatures and, with the exception of two points, the maximum scatter is about $\pm 10^{\circ}$ F about the mean. These predicted blade temperatures are well within the accuracy that would be required for practically all turbine applications. In figures 8(b) and (c) for the 0.250- and the 0.500-inch quadrant, the data scatter is about the same as in figure 8(a), but on an average the calculated blade temperatures more nearly agree with the measured temperatures.

The solid points in figure 8(a) were computed on the assumption that the heat is transferred to the water at a temperature T_6 rather than T_5 . These calculated blade temperatures are 30° to 50° F lower than those predicted with a coolant temperature of T_5 . This indicates that there is interference between the radially inward and outward flowing coolant within the blade passage, which results in heat transfer predictable only on the basis of a coolant-passage temperature T_5 .

Calculated turbine-blade trailing-edge temperatures. - The temperature near the trailing-edge coolant passage (thermocouple 3 in fig. 4) was also calculated and is shown in figure 9. Because the trailing-edge passage was 0.100 inch in diameter in all quadrants, the quadrant would not be expected to have a significant effect on the calculated trailing-edge temperature. There is some effect, however, because the division of total blade heat flow to the two blade passages is different for different quadrants. For example, in the 0.500-inch quadrant, a greater proportion of the total blade heat flow goes to the leading-edge passage than in the quadrant where the leading-edge passage is 0.125 inch in diameter.

Figure 9 shows the comparison between calculated and measured trailing-edge temperatures for the quadrants with 0.125-, 0.250-, and 0.500-inch-diameter leading-edge passages. The data scatter about the line for 1:1 correlation, but the scatter is roughly twice as great as it was for the leading-edge passages. For the 0.125-inch quadrant (fig. 7(a)), the calculated temperatures were all lower than the measured temperatures. This effect is not shown at the trailing edge, even though the coolant-passage diameter is only 0.100 inch. The calculated trailing-edge blade temperatures of the 0.125-inch quadrant are higher than the measured temperatures. As shown earlier, when the actual peripheral variation of the outside heat-transfer coefficient is considered, a higher

proportion of the total heat flow is transferred to the fluid in the leading-edge coolant passage. The difference shown by such calculations would improve the agreement of the calculated values with the measured values for the temperature near both the leading- and the trailing-edge passages in the 0.125-inch quadrant, but the magnitude of the change is not sufficient to bring the temperatures into 1:1 agreement. Therefore, it is unlikely that the results for the 0.125-inch quadrant are due, to any large degree, to the heat-flow distribution established by the analog constructed with a constant outside coefficient. In addition, the trend in the 0.125-inch quadrant was not obtained in either the 0.250- or the 0.500-inch quadrant.

Since the calculated temperatures agree with the measured temperatures near the trailing edge in the three quadrants checked, the coolant temperatures assumed in these passages are adequate.

Boundary-layer thickness. - A qualitative check of the restriction of the coolant flow within the blade coolant passages was made. The interference between the fluid streams flowing radially outward and inward within the same passage was indicated by the thickness of the boundary layer formed by the heated coolant flowing radially inward as calculated from equation (27) of reference 5. Of the particular points checked, the maximum calculated displacement thickness (equivalent thickness for constant velocity in the boundary layer) was 0.032 inch in the 0.100-inch passage. This forms an annulus that is about 87 percent of the passage cross-sectional area. As seen from the results of the comparison of calculated with measured blade temperatures, this degree of restriction of the coolant flow into the passage does not result in blade temperatures appreciably different from those predicted by available theory.

Use and Limitations of Theoretical Natural-Convection

Heat-Transfer Correlations

From the results presented thus far, a direct experimental proof has not been obtained that the theoretical natural-convection heat-transfer correlation presented in reference 5 is accurate for coolant-passage diameters from 0.100 to 0.500 inch (length-to-diameter ratios from 25.5 to 5.1). With the use of this correlation and corrections for the temperature differences due to the conduction process in the blade metal, however, it is indicated that blade temperatures can be predicted with sufficient accuracy for most engineering applications when coolants that give high heat-transfer coefficients, such as water, are used. The effects of even smaller diameter (larger length-to-diameter ratio) coolant passages still require investigation. The data obtained for this turbine show that coolant-flow restriction due to boundary-layer growth

with natural convection does not result in serious error in blade-temperature calculation and that use of the theoretical equation of reference 5 does not result in serious error in temperature calculation where passages of length-to-diameter ratio less than or equal to 25.5 are used.

In the present investigation the blade temperature range was limited by the coolant boiling temperature. In liquid-cooled turbines, it is desirable to operate at blade temperatures of 1000°F or higher depending on the turbine material. With these higher blade temperatures, metal strength is still high and the quantity of heat rejected from the engine cycle due to turbine cooling is reduced. Operation at these higher temperatures requires the use of coolants with high boiling points, such as the liquid metals, metal salts, and metal hydroxides, or water at supercritical pressures.

This experimental investigation did not give information concerning possible accuracy in calculating blade temperatures at higher temperature levels. An indication of possible errors to be expected is shown in figure 10. Blade temperature is plotted against the coolant core temperature obtained analytically for a range of coolant core temperatures from 200° to 1000°F . The blade temperature was taken to be the temperature at a point similar to the position of thermocouple 1 in figure 4. The temperature T_1 was calculated for the leading-edge part of the blades having 0.250-inch-diameter leading-edge coolant passages, using water as the coolant at a pressure of about 4000 pounds per square inch so that boiling of the coolant up to the critical temperature is prevented. Properties of the coolant at this condition were obtained from references 7, 9, 10, and 11. The blade-to-coolant heat-transfer coefficient was obtained from the natural-convection correlation of reference 5, and the Nusselt number was varied ± 50 percent from the value obtained by the correlation. The gas temperature for heat transfer was chosen as 1850°F , with a constant outside heat-transfer coefficient of $0.0556\text{ Btu}/(\text{sec})(\text{sq ft})(^{\circ}\text{F})$ ($200\text{ Btu}/(\text{hr})(\text{sq ft})(^{\circ}\text{F})$), which is considered average for present-day turbine designs. For the entire range of calculations, a ± 50 percent error in Nusselt number will affect the calculated blade temperatures by no more than 30°F . This error is well within the accuracy required for most engineering applications.

To determine the effect of a higher outside heat-transfer coefficient on the error caused by a ± 50 percent error in the assumption of the Nusselt number, calculations similar to those made for figure 10 were repeated for a range of coolant core temperatures from 400° to 500°F for an outside heat-transfer coefficient of $0.1389\text{ Btu}/(\text{sec})(\text{sq ft})(^{\circ}\text{F})$ ($500\text{ Btu}/(\text{hr})(\text{sq ft})(^{\circ}\text{F})$), which might be attained in a turbine with a very high mass flow. It was found that the error band was quite similar to that determined for the lower coefficient.

The errors of ± 50 percent in Nusselt number shown in figure 10 are estimated to cover a range large enough to permit use of the correlation of reference 5 for passage length-to-diameter ratios up to at least 25.5. Even larger variations, which might be encountered with smaller diameter passages, should not have a large effect on calculated blade temperature because of the relative insensitiveness of the calculations to Nusselt number so long as coolants with high heat-transfer coefficients are used.

SUMMARY OF RESULTS

An investigation of the effect of coolant-passage length-to-diameter ratio on natural-convection heat transfer in water-cooled turbine blades produced the following results:

1. Very high heat-transfer coefficients and small temperature differences between coolant and passage surface were characteristic of this turbine. Because of the errors associated with the measurement of temperature, errors in the small temperature difference were quite large. As a result, no differences in the nondimensional heat-transfer correlation could be shown for the various length-to-diameter ratios investigated.

2. A theoretical natural-convection correlation for flat plates and tubes of small length-to-diameter ratio was found to be adequate to define the heat-transfer coefficients for purposes of blade-temperature calculation. It was possible to calculate turbine blade temperatures near the leading-edge coolant passages within about 15° F at blade temperatures of approximately 300° F without regard to length-to-diameter ratio for values of this ratio from 25.5 to 5.1. There was a larger scatter in the calculated results for temperatures near the trailing-edge coolant passage of 0.100-inch diameter.

3. It was shown analytically for blade temperatures up to 1270° F that errors of ± 50 percent in the theoretical natural-convection Nusselt number would result in errors of less than 30° F in calculated blade temperatures for high heat-transfer coolants, such as water.

4. Because of the large temperature gradients within liquid-cooled turbine blades, it is necessary to take into account the temperature differences between the coolant-passage surface and the place of measurement in order to calculate local blade-metal temperatures or to use experimental data to obtain heat-transfer correlations.

Lewis Flight Propulsion Laboratory
National Advisory Committee for Aeronautics
Cleveland, Ohio, October 27, 1955

APPENDIX A

SYMBOLS

A	area, sq ft
b	length of blade coolant passage, ft
c_p	specific heat of coolant at constant pressure, Btu/(lb)(°F)
D	diameter, ft
f	function
Gr	Grashof number, $\frac{\omega^2 r \rho^2 \beta \theta l^3}{\mu^2}$
h	heat-transfer coefficient, Btu/(sec)(sq ft)(°F)
k	thermal conductivity, Btu/(sec)(ft)(°F)
k_m	thermal conductivity, blade and rotor rim material, 0.00439 Btu/(sec)(ft)(°F)
l	length of coolant passage in blade and rotor rim, ft
Nu	Nusselt number, hl/k
Pr	Prandtl number, $c_p \mu / k$
Q	heat-flow rate, Btu/sec
r	radius, ft
T	temperature, °F
w	weight-flow rate, lb/sec
β	coefficient of thermal expansion of coolant, 1/°F
θ	temperature difference, $T_5 - T_{i,le}$ or $T_5 - T_{i,te}$, °F
Φ	temperature difference between outer and inner turbine rim thermocouples, °F
μ	dynamic viscosity of coolant, lb/(sec)(ft)

ρ density of coolant, lb/cu ft
 τ metal thickness, ft
 ω angular velocity, radians/sec
 ψ analog correction factor defined in appendix B

Subscripts:

a arbitrary location
B blade
c coolant
i inside (coolant passage)
in inlet
le leading-edge part of blade
R rim
T total
te trailing-edge part of blade
1 to 6 thermocouple locations (see fig. 4)

APPENDIX B

COOLANT-PASSAGE WALL TEMPERATURE CORRECTIONS

The following equation from reference 12 defines the heat flow through a tube when the outer and inner walls have different temperatures:

$$Q = k \frac{2\pi b}{\ln \frac{r_a}{r_i}} (T_i - T_a)$$

Rearranging terms yields

$$T_i - T_a = \frac{Q}{k2\pi b} \ln \frac{r_a}{r_i} \quad (1)$$

This equation states that the temperature difference in a tube of length b depends on the radius and the heat flow.

For the case of a cylindrical passage in a noncylindrical body, as in a liquid-cooled turbine blade, it is apparent that this equation is not valid, since the passage is surrounded by nonconcentric isotherms. In the present investigation, equation (1) is modified by a correction factor to account for the nonconcentricity of the isotherms. The equation is then valid only locally and, because of this restriction, the correction factor must be determined for specific locations on specific configurations.

Since electrical analogs have been used previously in turbine-blade temperature studies (ref. 13), such a device was constructed to determine the correction factors needed in this investigation. For construction of the analog, the outside heat-transfer coefficient was assumed on the basis of average over-all values from the entire experimental range. For the inside heat-transfer coefficient, an estimate was made. The accuracy of the estimate was considered adequate, since the heat flow is largely determined by the outside heat-transfer coefficient.

Since the correction was desired in the form

$$T_i - T_a = \psi Q \frac{\ln \frac{r_a}{r_i}}{k_m 2\pi b} \quad (2)$$

the correction factor ψ was determined as

$$\psi = \frac{\left(\frac{T_i - T_a}{Q}\right)_{\text{analog}}}{\left(\frac{T_i - T_a}{Q}\right)_{\text{calculated}}}$$

where $\left(\frac{T_i - T_a}{Q}\right)_{\text{analog}}$ is measured from the analog and $\left(\frac{T_i - T_a}{Q}\right)_{\text{calculated}}$ is calculated from equation (1).

The first analog constructed was 10 times the blade size and was fabricated of 24-gage chromel wire in a 1/2- by 1/2-inch grid. The locations of the thermocouples in the actual blade were represented as accurately as the grid spacing would permit, since the thermocouple locations in the analog must occur at grid junctions. On the basis of approximate calculations of the thermal resistance of the enclosed ceramic-insulated thermocouple assembly, the thermocouple installation in the blade was simulated by an electrical resistance 100 times that of the same span of the normal analog wire.

Although the 10-times-size analog allowed the placement of thermocouples accurately enough for the leading-edge part of the analog, it was found that the thermocouples in the trailing-edge portion of the analog could not be placed with required accuracy, owing to the relatively few grid junctions in that thin-section region of the analog. Consequently, a 20-times-size analog of the trailing-edge part of the turbine blade was constructed. This analog is shown in figure 11. The extent of the trailing-edge part of the blade (the curved left grid extremity in fig. 11) was determined by establishing the line across which there is a zero temperature gradient on the 10-times-size analog for the blades that have 0.250-inch-diameter leading-edge coolant passages. That particular blade type was chosen for the design of the 20-times-size analog because its zero-thermal-gradient line fell between and well represented those of the other blade types for which analogs were constructed. No analog was constructed for the blades with a 0.375-inch-diameter coolant passage because no additional information would be gained.

REFERENCES

1. Eckert, E. R. G., Diaguila, Anthony J., and Curren, Arthur N.: Experiments on Mixed-Free- and -Forced-Convective Heat Transfer Connected with Turbulent Flow Through a Short Tube. NACA TN 2974, 1953.

2. Eckert, E. R. G., Diaguila, Anthony J., and Livingood, John N. B.: Free-Convection Effects on Heat Transfer for Turbulent Flow Through a Vertical Tube. NACA TN 3584, 1955.
3. Freche, John C., and Diaguila, A. J.: Heat-Transfer and Operating Characteristics of Aluminum Forced-Convection and Stainless-Steel Natural-Convection Water-Cooled Single-Stage Turbines. NACA RM E50D03a, 1950.
4. Diaguila, Anthony J., and Freche, John C.: Blade-to-Coolant Heat-Transfer Results and Operating Data from a Natural-Convection Water-Cooled Single-Stage Turbine. NACA RM E51I17, 1951.
5. Eckert, E. R. G., and Jackson, Thomas W.: Analytical Investigation of Flow and Heat Transfer in Coolant Passages of Free-Convection Liquid-Cooled Turbines. NACA RM E50D25, 1950.
6. Livingood, John N. B., and Brown, W. Byron: Analysis of Temperature Distribution in Liquid-Cooled Turbine Blades. NACA Rep. 1066, 1952. (Supersedes NACA TN 2321.)
7. Keenan, Joseph H., and Keyes, Frederick G.: Thermodynamic Properties of Steam. John Wiley & Sons, Inc., 1936.
8. McAdams, William H.: Heat Transmission. Second ed., McGraw-Hill Book Co., Inc., 1942.
9. Sigwart, K.: Messungen der Zähigkeit von Wasser und Wasserdampf bis ins kritische Gebiet. Forsch. Geb. Ing.-Wes., Bd. 7, Heft 3, May/June 1936, pp. 125-140.
10. Timrot, D. L.: Determination of the Viscosity of Steam and Water at High Temperatures and Pressures. Jour. Phys. (USSR), vol. 2, 1940, pp. 419-436.
11. Timrot, D. L., and Vargaftik, N. B.: Heat Conduction of Water at High Temperatures. Jour. Tech. Phys. (USSR), vol. X, no. 13, 1940, pp. 1063-1073.
12. Eckert, E. R. G.: Introduction to the Transfer of Heat and Mass. McGraw-Hill Book Co., Inc., 1950.
13. Ellerbrock, Herman H., Jr., Schum, Eugene F., and Nachtigall, Alfred J.: Use of Electric Analogs for Calculation of Temperature Distribution of Cooled Turbine Blades. NACA TN 3060, 1953.

TABLE I. - OPERATING DATA FOR WATER-COOLED TURBINE

Tur- bine speed, rpm	Effec- tive gas temper- ature, °F	Combus- tion gas flow, lb/sec per blade	Cool- ant flow, lb/sec per blade	Temperature ^a , °F								Outer rim	Inner rim
				Near lead- ing edge 1	Mid- chord 2	Near trail- ing edge 3	Trail- ing edge 4	Cool- ant inlet	Cool- ant at tip 5	Cool- ant out- let 6			
Leading-edge coolant-passage diameter, 0.125 in.													
4,000	524	0.107	0.022	194	207	181	220	70	125	82	(b)	(b)	
	559	.107	.016	207	220	193	241	70	135	94			
	586	.108	.013	215	227	201	250	70	140	100			
	561	.108	.010	217	230	205	250	71	146	108			
	557	.108	.0083	222	233	211	256	71	150	114			
	543	.108	.0052	238	245	224	265	68	175	137			
	538	.108	.0032	255	267	250	284	76	202	175			
4,000	767	.109	.022	257	272	242	305	70	154	95			
	730	.109	.016	255	273	245	300	70	163	108			
	749	.108	.013	265	282	255	310	71	175	118			
	864	.107	.010	272	316	293	355	73	207	142			
	724	.109	.0084	287	289	262	317	72	192	140			
	721	.108	.0052	292	310	285	335	72	225	175			
	751	.108	.0032	336	335	320	351	76	270	215			
6,000	858	.106	.022	257	275	245	306	73	163	116			
	811	.106	.015	255	273	245	305	74	165	122			
	826	.106	.013	274	282	255	319	74	190	132			
	816	.106	.010	282	287	260	320	75	195	145			
	844	.106	.0085	296	302	274	335	76	210	162			
	831	.106	.0052	327	330	301	357	81	244	203			
	821	.110	.0043	340	344	317	365	87	262	217			
8,000	858	.108	.022	267	267	234	290	69	152	104			
	824	.110	.015	270	275	246	295	75	170	127			
	847	.110	.013	288	293	257	318	86	194	142			
	825	.104	.010	294	302	261	320	77	211	157			
	867	.100	.0083	305	310	277	325	71	212	169			
	847	.114	.0052	335	339	310	350	72	255	210			
10,000	858	.111	.022	252	280	242	280	74	160	112			
	831	.110	.015	275	291	255	289	74	177	130			
	862	.110	.013	300	302	265	305	75	192	148			
	827	.113	.010	297	302	266	302	76	197	157			
	833	.111	.0082	310	321	283	322	76	215	180			
	845	.110	.0052	335	347	---	347	74	246	209			
10,000	1012	.110	.022	302	319	---	325	72	177	119			
	1023	.110	.016	332	335	---	339	72	200	144			
	1026	.110	.012	324	350	---	352	74	213	164			
	1040	.113	.010	321	350	---	355	71	219	167			
	1029	.112	.0085	327	356	---	353	72	227	180			
	1030	.113	.0073	335	368	---	350	72	237	193			
10,000	1227	.112	.022	344	313	---	359	72	201	135			
	1221	.113	.016	367	330	---	377	72	220	160			
	1222	.113	.013	369	336	---	382	72	239	180			

^aNumbered thermocouples refer to thermocouples of fig. 4; others to thermocouples of fig. 2.

^bNo thermocouple here in this quadrant.

TABLE I. - Continued. OPERATING DATA FOR WATER-COOLED TURBINE

Tur- bine speed, rpm	Effec- tive gas temper- ature, °F	Combus- tion gas flow, lb/sec per blade	Cool- ant flow, lb/sec per blade	Temperature ^a , °F								Outer rim	Inner rim
				Near lead- ing edge 1	Mid- chord 2	Near trail- ing edge 3	Trail- ing edge 4	Cool- ant inlet	Cool- ant at tip 5	Cool- ant out- let 6			
Leading-edge coolant-passage diameter, 0.250 in.													
4,000	524	0.107	0.022	151	177	169	(b)	70	94	85	120	91	
	559	.107	.016	161	188	190		70	105	97	133	100	
	586	.108	.013	166	195	197		70	109	102	139	107	
	561	.108	.010	170	197	198		71	122	111	144	115	
	557	.108	.0083	175	202	201		71	129	121	150	122	
	543	.108	.0052	193	220	221		68	152	150	172	147	
	538	.108	.0032	218	242	246		76	185	182	200	181	
4,000	767	.109	.022	188	232	227	70	114	98	151	105		
	730	.109	.016	192	233	232	70	130	113	160	116		
	749	.108	.013	200	244	243	71	138	120	168	125		
	864	.107	.010	229	281	280	73	162	147	198	150		
	724	.109	.0084	211	252	252	72	155	144	185	145		
	721	.108	.0052	237	275	277	72	190	180	213	177		
	751	.108	.0032	281	315	318	76	232	219	253	224		
6,000	858	.106	.022	192	242	228	73	125	108	156	110		
	811	.106	.015	200	247	235	74	139	125	169	125		
	826	.106	.013	209	255	246	74	146	136	178	136		
	816	.106	.010	215	262	254	75	157	150	188	148		
	844	.106	.0085	231	278	269	76	175	167	204	162		
	831	.106	.0052	268	311	302	81	214	210	240	207		
	821	.110	.0043	282	326	319	87	228	222	255	222		
8,000	858	.108	.022	191	240	225	69	120	105	151	107		
	824	.110	.015	205	254	235	75	140	132	174	130		
	847	.110	.013	227	272	255	86	155	146	192	144		
	825	.104	.010	233	277	265	77	166	160	204	156		
	867	.100	.0083	238	287	275	71	180	173	211	168		
	847	.114	.0052	285	320	317	72	215	212	255	212		
10,000	858	.111	.022	200	257	227	74	125	114	165	115		
	831	.110	.015	212	265	237	74	142	135	179	133		
	862	.110	.013	225	282	253	75	157	150	193	147		
	827	.113	.010	230	285	260	76	157	164	201	160		
	833	.111	.0082	247	300	279	76	167	186	223	181		
	845	.110	.0052	278	332	316	74	190	220	255	220		
10,000	1012	.110	.022	225	292	260	72	122	122	178	122		
	1023	.110	.016	242	309	279	72	140	150	200	146		
	1026	.110	.012	258	325	295	74	151	170	219	165		
	1040	.113	.010	270	328	308	71	161	191	238	185		
	1029	.112	.0085	292	350	325	72	183	213	257	210		
	1030	.113	.0073	304	358	335	72	192	222	266	222		
10,000	1227	.112	.022	258	332	300	72	131	139	209	140		
	1221	.113	.016	277	352	320	72	146	168	235	165		
	1222	.113	.013	292	364	336	72	161	187	251	184		

^aNumbered thermocouples refer to thermocouples of fig. 4; others to thermocouples of fig. 2.

^bNo thermocouple here in this quadrant.

TABLE I. - Continued. OPERATING DATA FOR WATER-COOLED TURBINE

Tur- bine speed, rpm	Effec- tive gas temper- ature, °F	Combus- tion gas flow, lb/sec per blade	Cool- ant flow, lb/sec per blade	Temperature ^a , °F								Outer rim	Inner rim
				Near lead- ing edge 1	Mid- chord 2	Near trail- ing edge 3	Trail- ing edge 4	Cool- ant inlet	Cool- ant at tip 5	Cool- ant out- let 6			
Leading-edge coolant-passage diameter, 0.375 in.													
4,000	524	0.107	0.022	143	155	177	(b)	70	95	87	(b)	(b)	
	559	.107	.016	150	164	187		70	100	92			
	586	.108	.013	160	175	200		70	109	104			
	561	.108	.010	165	178	203		71	116	113			
	557	.108	.0083	170	183	207		71	124	120			
	543	.108	.0052	187	200	225		68	150	145			
	538	.108	.0032	213	227	250		76	180	177			
4,000	767	.109	.022	182	203	235		70	108	101			
	730	.109	.016	182	200	230		70	113	105			
	749	.108	.013	195	217	248		71	127	123			
	864	.107	.010	225	250	284		73	155	150			
	724	.109	.0084	205	227	258		72	150	145			
	721	.108	.0052	233	252	282		72	185	180			
	751	.108	.0032	272	293	318		76	225	212			
6,000	858	.106	.022	182	205	234		73	112	105			
	811	.106	.015	194	216	244		74	130	127			
	826	.106	.013	201	225	251		74	140	137			
	816	.106	.010	209	232	258		75	151	149			
	844	.106	.0085	224	249	275		76	169	165			
	831	.106	.0052	257	280	303		81	210	204			
	821	.110	.0043	268	292	317		87	225	213			
8,000	858	.108	.022	183	210	233		69	119	111			
	824	.110	.015	196	220	244		75	136	132			
	847	.110	.013	209	240	258		86	157	152			
	825	.104	.010	215	247	263		77	167	162			
	867	.100	.0083	227	253	277		71	177	172			
	847	.114	.0052	262	288	309		72	223	215			
10,000	858	.111	.022	188	216	243		74	127	120			
	831	.110	.015	197	225	251		74	140	136			
	862	.110	.013	212	240	263		75	155	152			
	827	.113	.010	219	247	275		76	167	164			
	833	.111	.0082	238	264	293		76	190	185			
	845	.110	.0052	264	289	320		74	220	209			
10,000	1012	.110	.022	209	239	281		72	135	126			
	1023	.110	.016	223	252	295		72	152	147			
	1026	.110	.012	237	269	309		74	171	165			
	1040	.113	.010	251	280	317		71	189	183			
	1029	.112	.0085	262	287	325		72	202	197			
	1030	.113	.0073	277	302	338		72	218	211			
10,000	1227	.112	.022	240	276	322		72	151	144			
	1221	.113	.016	260	294	337		72	175	168			
	1222	.113	.013	278	310	355		72	195	187			

^aNumbered thermocouples refer to thermocouples of fig. 4; others to thermocouples of fig. 2.

^bNo thermocouple here in this quadrant.

TABLE I. - Concluded. OPERATING DATA FOR WATER-COOLED TURBINE

Tur- bine speed, rpm	Effec- tive gas temper- ature, °F	Combust- ion gas flow, lb/sec per blade	Cool- ant flow, lb/sec per blade	Temperature ^a , °F								Outer rim	Inner rim
				Near lead- ing edge 1	Mid- chord 2	Near trail- ing edge 3	Trail- ing edge 4	Cool- ant inlet	Cool- ant at tip 5	Cool- ant out- let 6			
Leading-edge coolant-passage diameter, 0.500 in.													
4,000	524	0.107	0.022	137	147	165	190	70	89	85	(b)	(b)	
	559	.107	.016	150	160	180	202	70	100	96			
	586	.108	.013	157	170	190	215	70	105	105			
	561	.108	.010	161	172	194	217	71	111	110			
	557	.108	.0083	165	176	200	220	71	130	118			
	543	.108	.0052	180	197	222	232	68	150	148			
	538	.108	.0032	212	225	250	275	76	185	177			
4,000	767	.109	.022	172	193	227	310	70	106	98			
	730	.109	.016	180	194	225	310	70	110	107			
	749	.108	.013	188	210	242	317	71	129	125			
	864	.107	.010	213	243	273	367	73	152	151			
	724	.109	.0084	202	218	252	334	72	140	142			
	721	.108	.0052	227	247	275	346	72	185	180			
	751	.108	.0032	265	283	306	385	76	225	215			
6,000	858	.106	.022	183	207	220	279	73	125	120			
	811	.106	.015	185	208	222	277	74	129	125			
	826	.106	.013	192	218	230	283	74	139	137			
	816	.106	.010	201	226	240	287	75	158	150			
	844	.106	.0085	215	242	255	300	76	167	165			
	831	.106	.0052	252	273	282	320	81	211	204			
	821	.110	.0043	267	287	297	349	87	225	217			
8,000	858	.108	.022	173	204	210	290	69	116	111			
	824	.110	.015	187	217	217	254	75	135	132			
	847	.110	.013	200	232	232	268	86	153	147			
	825	.104	.010	207	242	242	284	77	166	162			
	867	.100	.0083	225	253	257	362	71	182	173			
	847	.114	.0052	257	286	286	393	72	227	210			
10,000	858	.111	.022	177	211	210	270	74	125	120			
	831	.110	.015	185	218	217	306	74	136	135			
	862	.110	.013	201	233	233	220	75	151	150			
	827	.113	.010	210	240	241	335	76	165	162			
	833	.111	.0082	227	260	260	370	76	182	183			
	845	.110	.0052	256	283	285	409	74	217	211			
10,000	1012	.110	.022	194	229	229	407	72	130	127			
	1023	.110	.016	209	243	243	425	72	147	146			
	1026	.110	.012	225	257	259	435	74	165	162			
	1040	.113	.010	228	268	270	448	71	185	180			
	1029	.112	.0085	250	283	283	458	72	206	198			
	1030	.113	.0073	258	292	292	464	72	215	210			
10,000	1227	.112	.022	214	260	259	500	72	148	144			
	1221	.113	.016	232	277	275	520	72	170	166			
	1222	.113	.013	246	287	283	525	72	187	181			

^aNumbered thermocouples refer to thermocouples of fig. 4; others to thermocouples of fig. 2.

^bNo thermocouple here in this quadrant.

TABLE II. - SUMMARY OF ELECTRICAL ANALOG RESULTS

Leading-edge coolant- passage diameter, in.	Trailing- edge coolant- passage diameter, in.	Fraction of total current flow through leading-edge coolant- passage walls	Fraction of total current flow through trailing-edge coolant- passage walls	Correc- tion factor, ψ_{le} (a)	Correc- tion factor, ψ_{te} (b)
0.125	0.100	0.576	0.424	0.755	-----
.250	.100	.613	.387	1.151	1.415
.500	.100	.647	.353	1.669	-----

^aThese analogs have a scale of 10 times blade size.

^bAnalog has a scale of 20 times blade size.

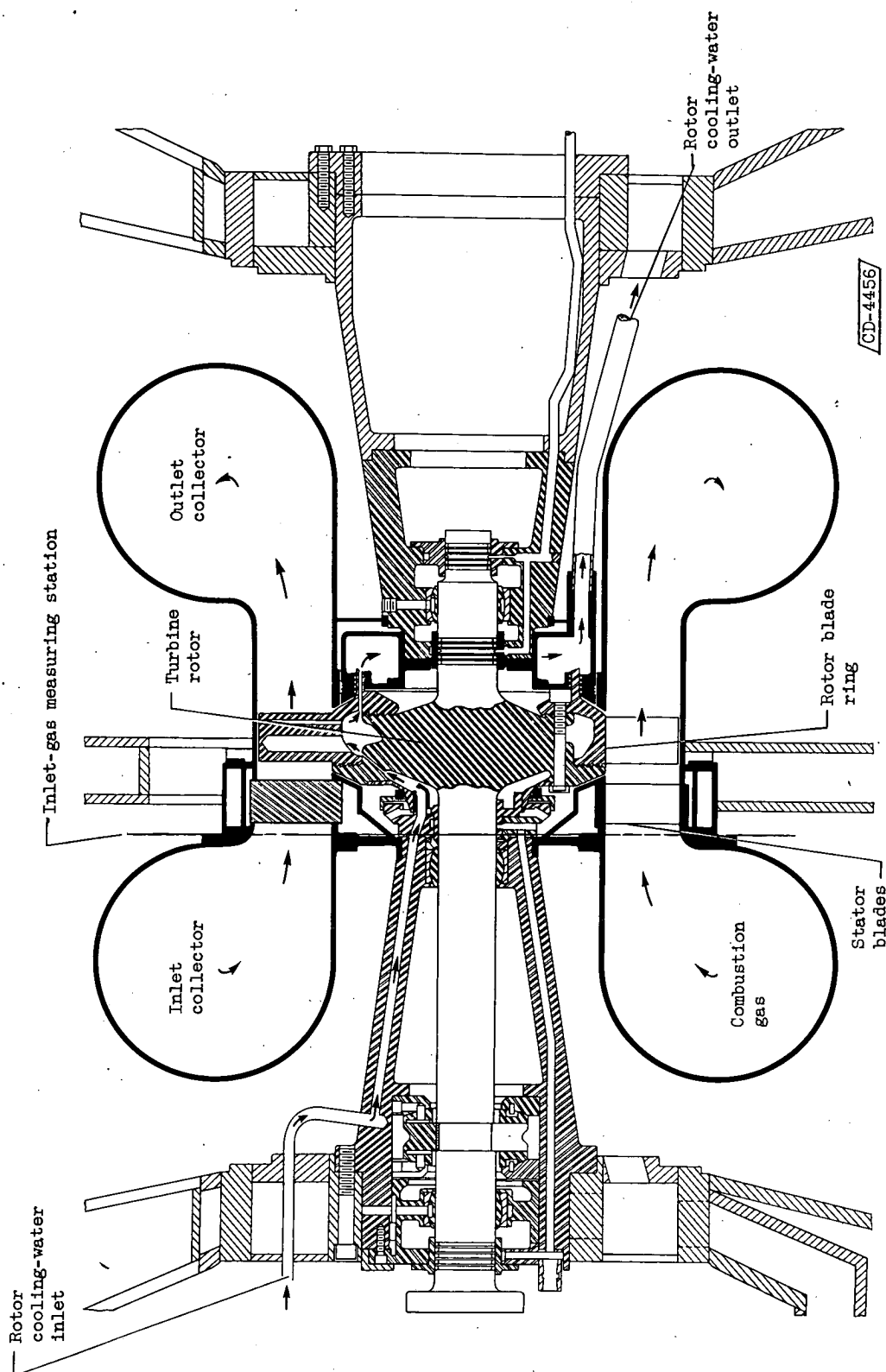


Figure 1. - Cross section of natural-convection liquid-cooled turbine.

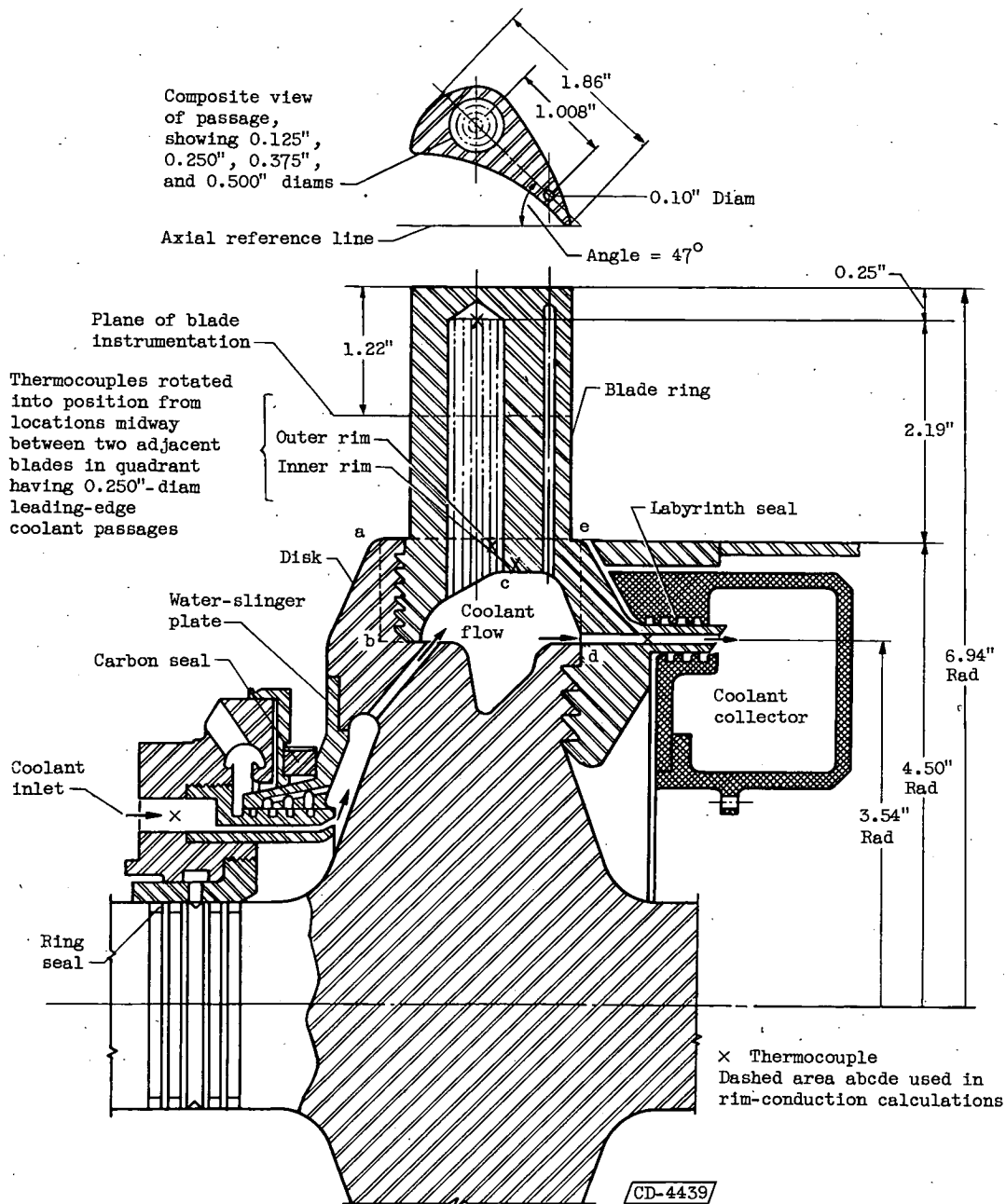


Figure 2. - Cross section of rotor and blade coolant system of natural-convection liquid-cooled turbine showing instrumentation locations.

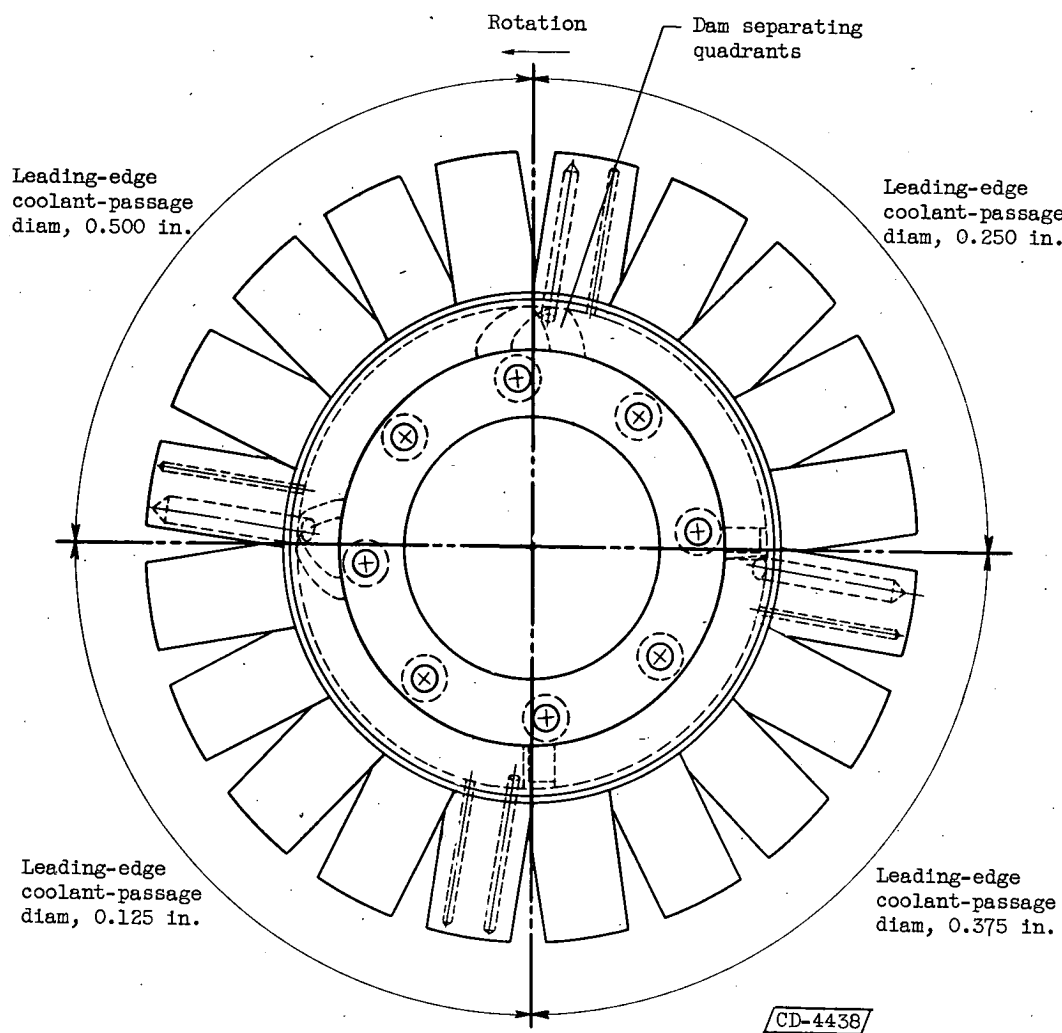


Figure 3. - Schematic diagram of turbine rotor showing quadrant division and dams for separating quadrant coolant.

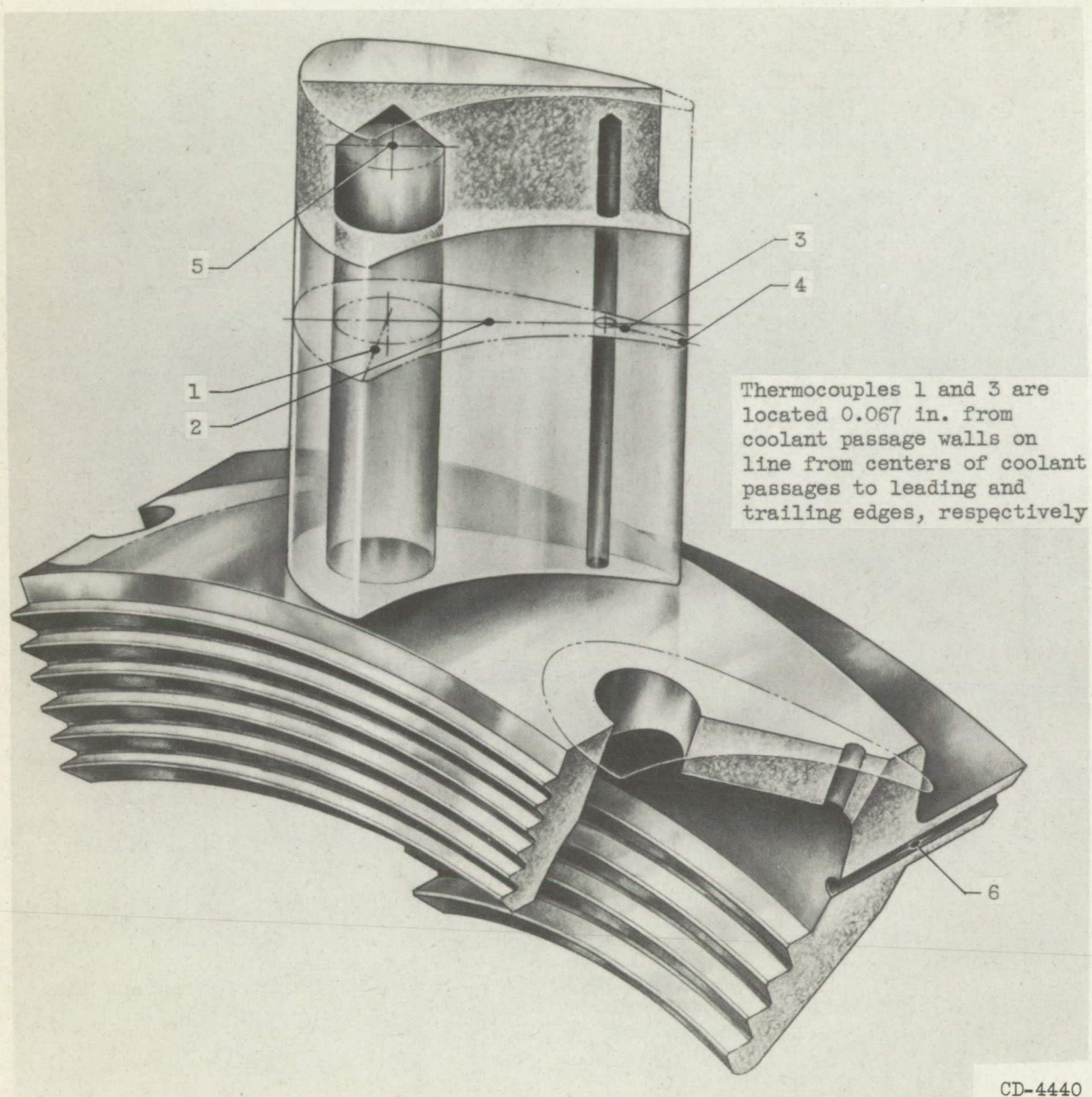
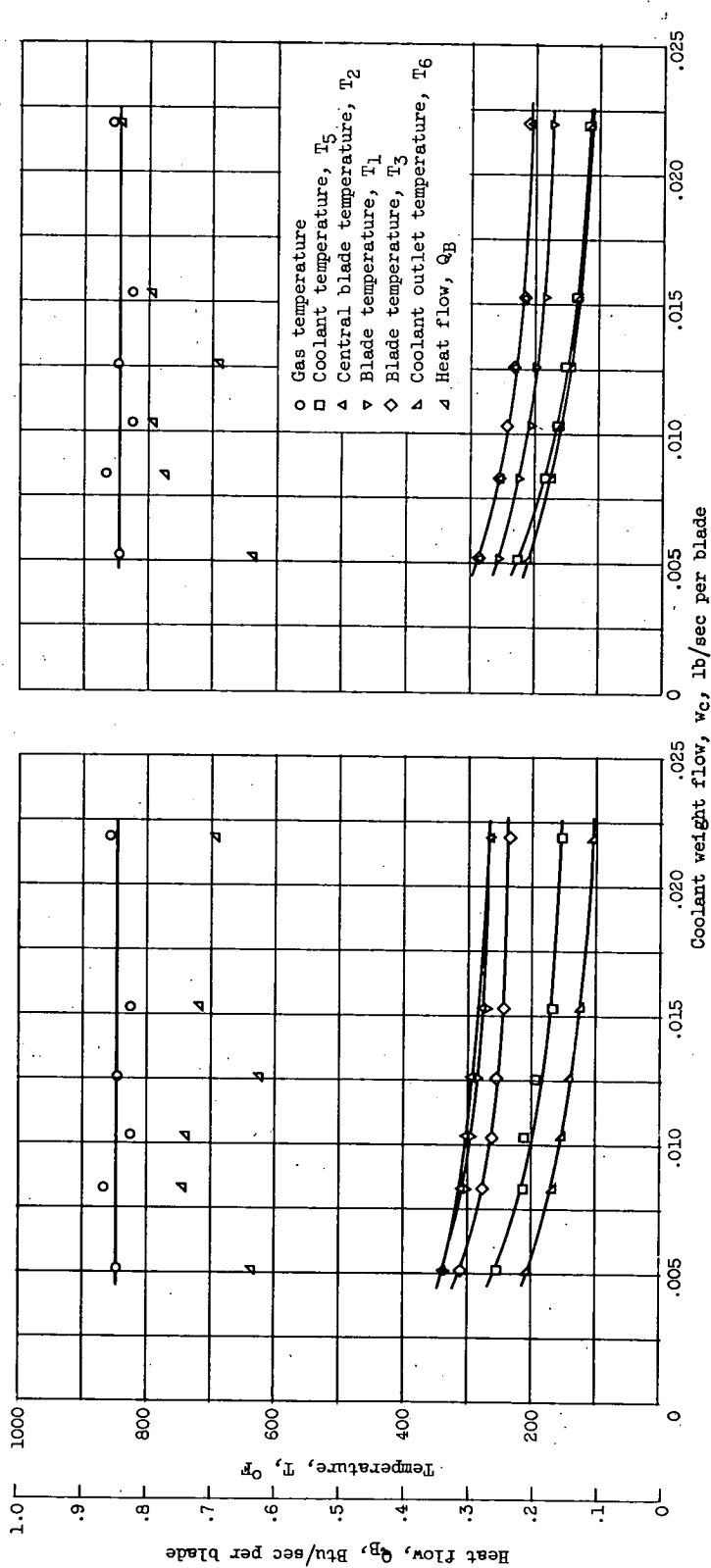


Figure 4. - Thermocouple locations on rotor blade of natural-convection liquid-cooled turbine.



(a) Leading-edge coolant-passage diameter, 0.125 inch. (b) Leading-edge coolant-passage diameter, 0.500 inch.

Figure 5. - Operating data for water-cooled turbine at rotor speed of 8000 rpm.

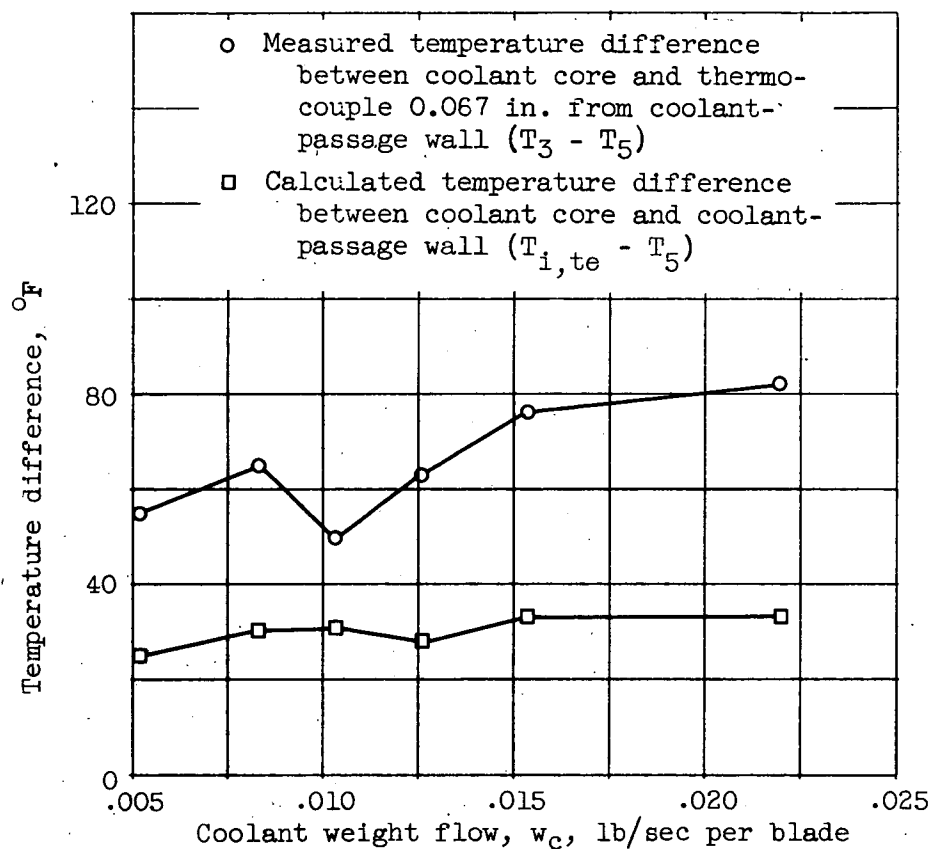


Figure 6. - Temperature differences for heat transfer for 0.100-inch-diameter trailing-edge coolant passages in blade quadrant with 0.125-inch-diameter leading-edge coolant passages at rotor speed of 8000 rpm.

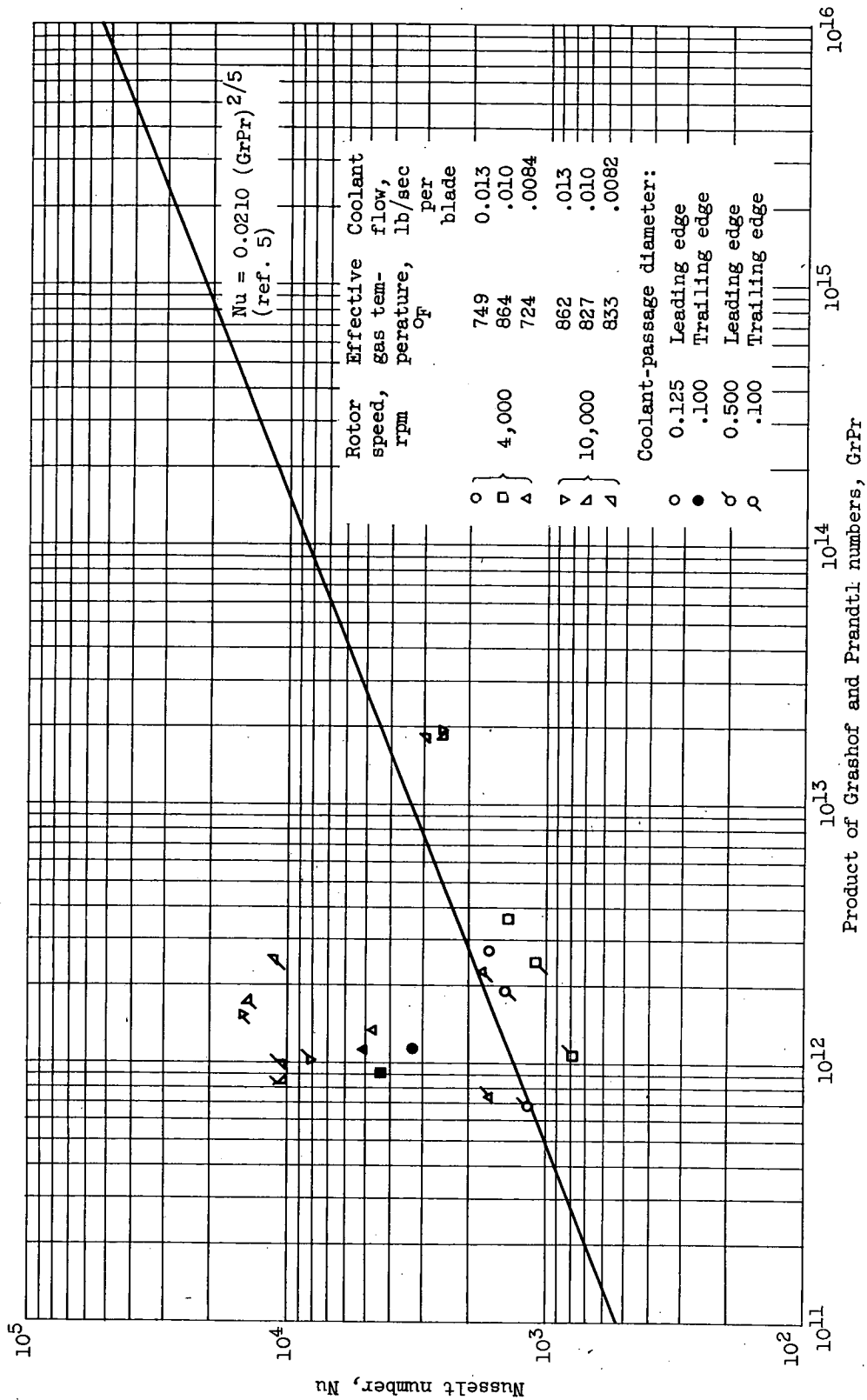
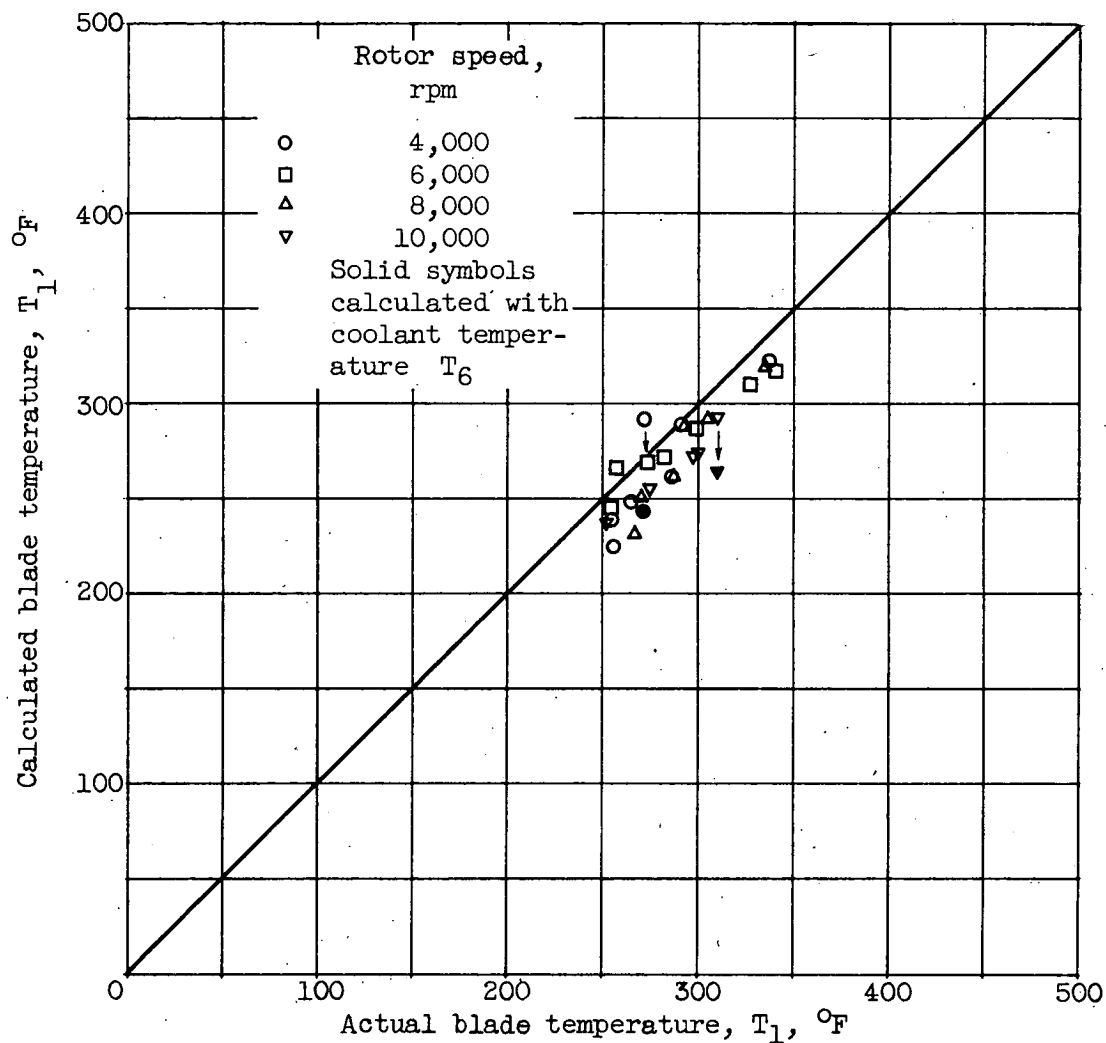
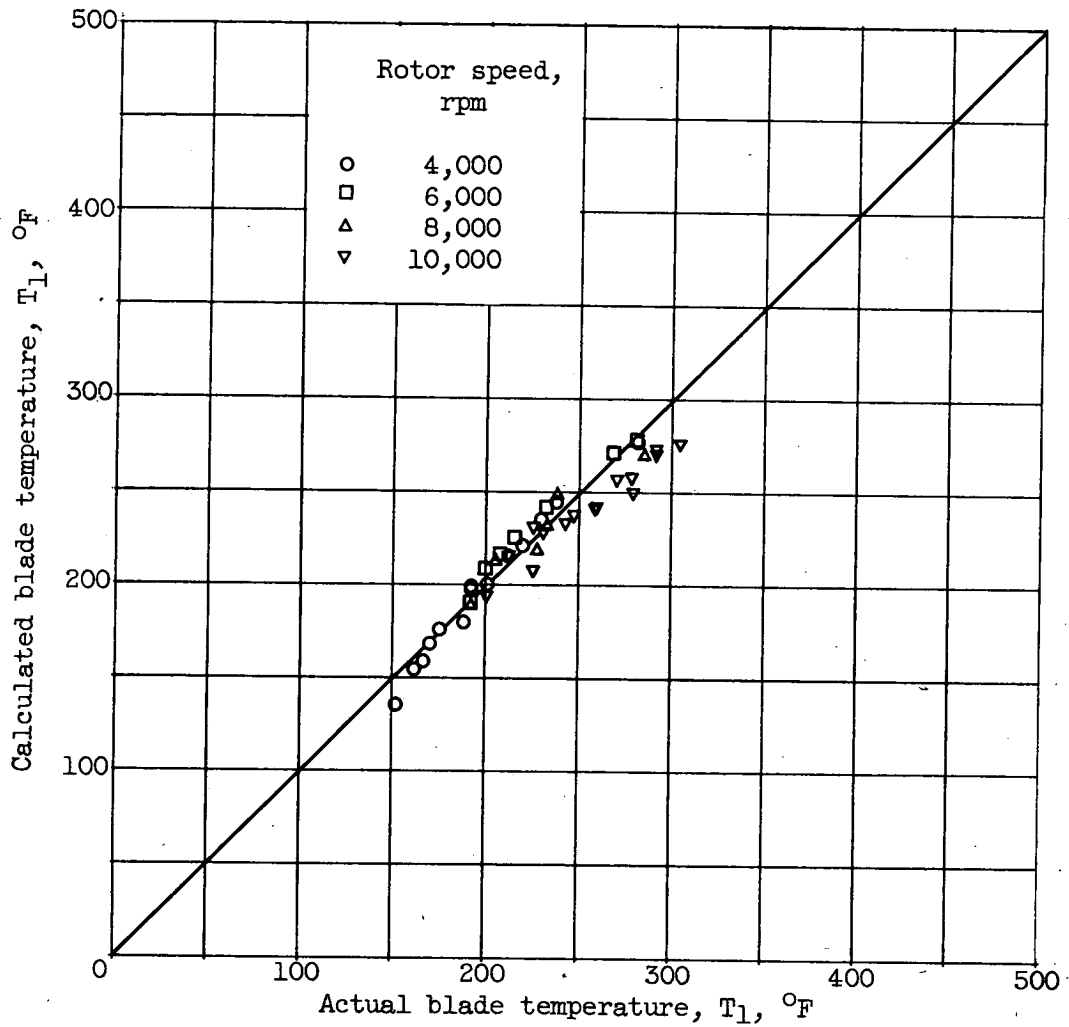


Figure 7. - Dimensionless heat-transfer correlation using calculated coolant-passage surface temperature.



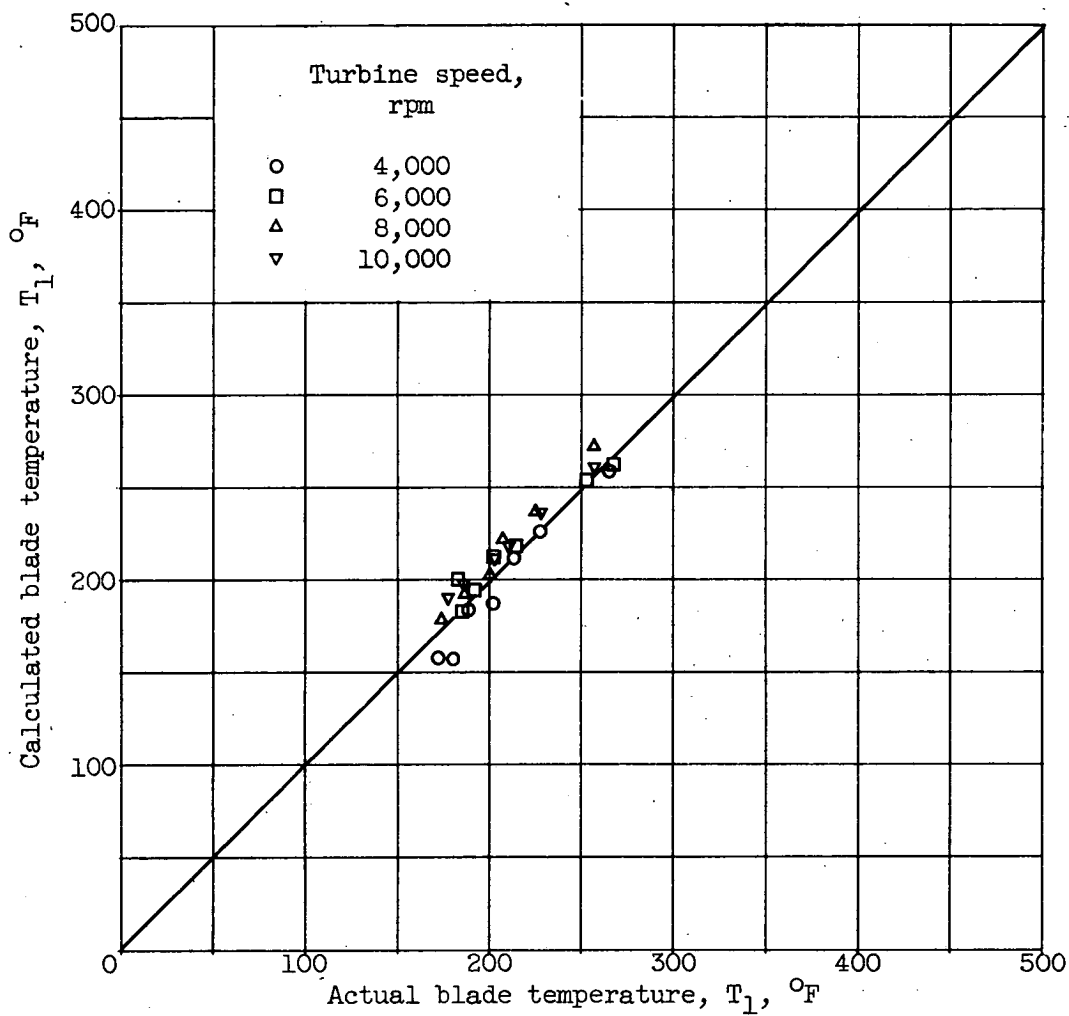
(a) Leading-edge coolant-passage diameter, 0.125 inch.

Figure 8. - Comparison of measured and calculated blade temperatures in leading-edge part of blades with water as coolant.



(b) Leading-edge coolant-passage diameter, 0.250 inch.

Figure 8. - Continued. Comparison of measured and calculated blade temperatures in leading-edge part of blades with water as coolant.



(c) Leading-edge coolant-passage diameter, 0.500 inch.

Figure 8. - Concluded. Comparison of measured and calculated blade temperatures in leading-edge part of blades with water as coolant.

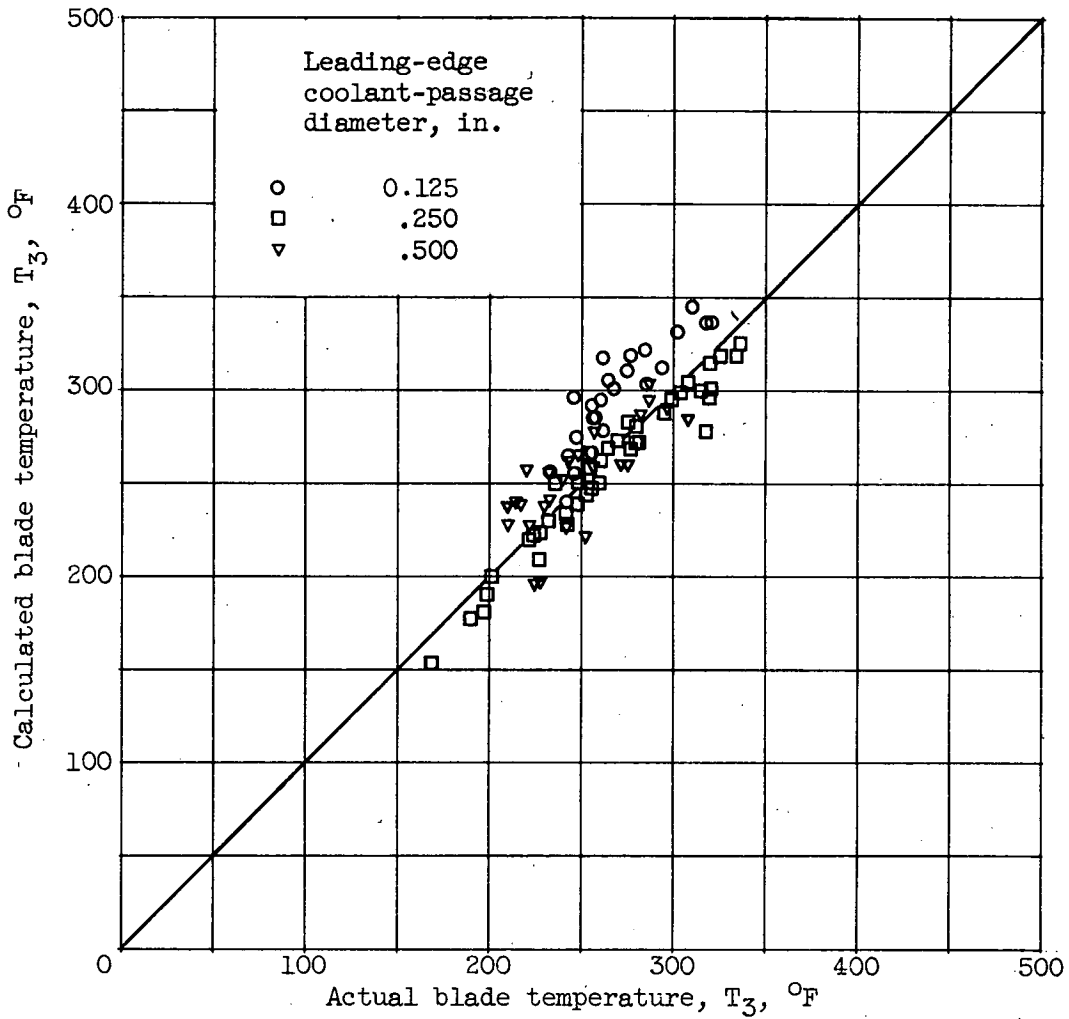


Figure 9. - Comparison of measured and calculated blade temperatures in trailing-edge part of blades with water as coolant for range of turbine speeds.

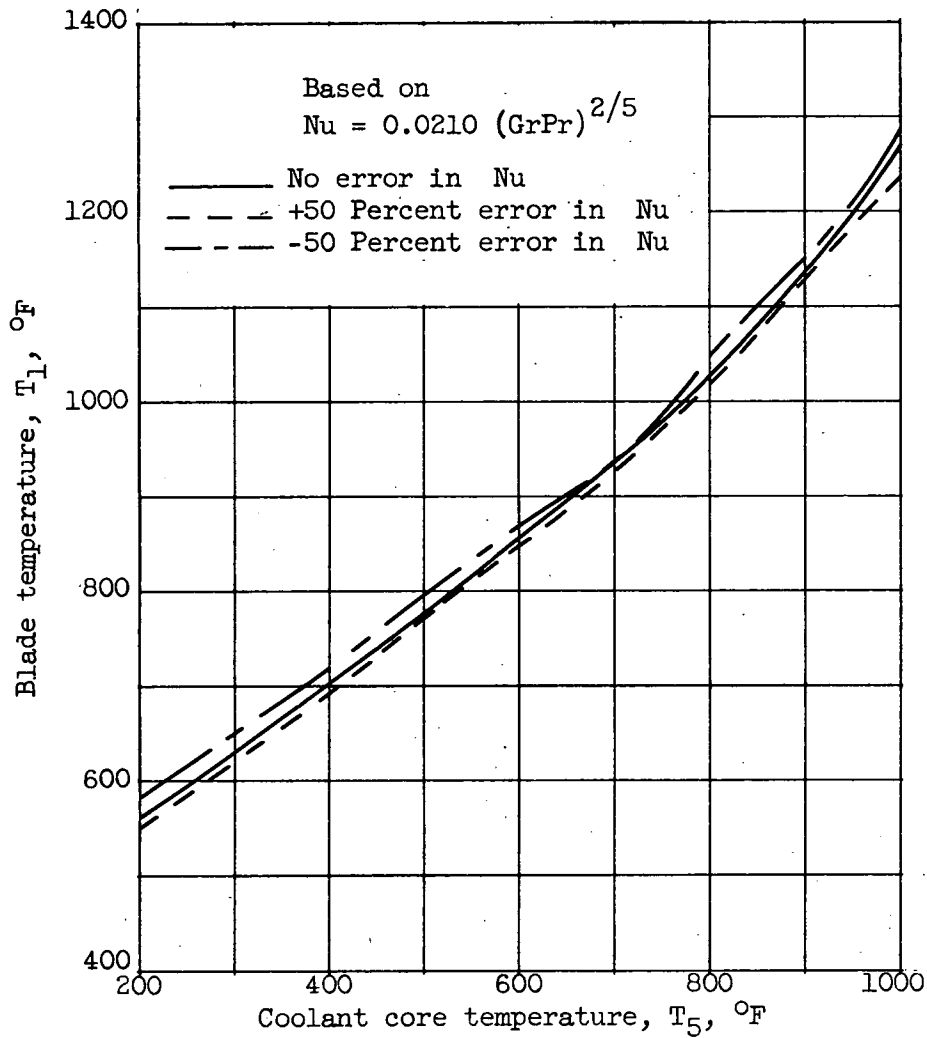


Figure 10. - Effect of error in assumption of Nusselt number on calculated blade temperature for natural-convection cooling with water. Effective gas temperature, 1850° F.

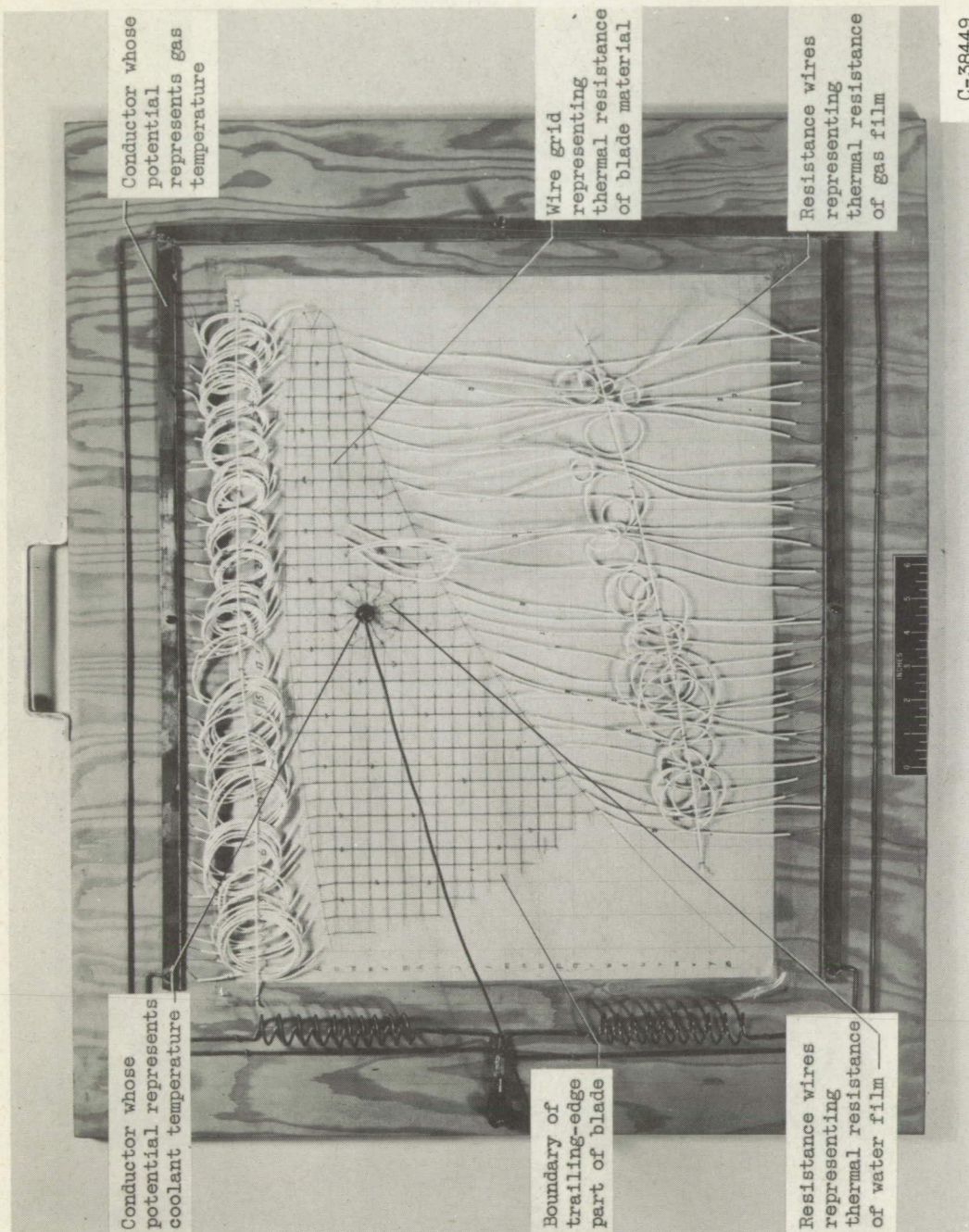


Figure 11. - Electrical analog of trailing-edge part of liquid-cooled turbine blade. X20 blade size.